

Effects of Machining Parameters on Performance Characteristics of Powder Mixed EDM of Inconel-800

S. Kumar^{1*} and A. K. Dhingra²

¹University Institute of Engineering & Technology, Maharshi Dayanand University, Rohtak-124001, Haryana, INDIA

*E-mail: itsarungarg@gmail.com

Phone: 09416741612

²Department of Mechanical Engineering, University Institute of Engineering & Technology, Maharshi Dayanand University, Rohtak-124001, Haryana, INDIA

Phone: 09541153059

ABSTRACT

This research work explores the connection of machining parameters, i.e. peak current (I_p), pulse on-time (T_{on}), pulse off-time (T_{off}), tool material (copper, copper-chromium, graphite) and powder particles (tungsten carbide, cobalt, boron carbide) on surface roughness (SR) for Inconel-800 superalloy in powder mixed electrical discharge machining process (PMEDM). The Box–Behnken design had been applied to design the experiments, and response surface methodology (RSM) was employed to cultivate the empirical models. Forty-six experiments were conducted as per Box-Behnken method of RSM. The results indicated that when current increases from 4 to 12 A, SR increases from 4.23 to 12.57 μm , while with the increase of T_{off} from 30 to 60 μs , SR decreased from 9.23 to 7.10 μm . Results also indicated that copper as a tool electrode and boron carbide as a powder additive has significantly effect on SR. The predicted results based on developed models are found to be in good agreement with the experimental results reasonably well with the coefficient of determination 0.96 for surface roughness. Furthermore, certain machined specimens were analyzed using energy-dispersive x-ray analysis (EDX) and scanning electron microscope (SEM) techniques.

Keywords: Powder mixed electrical discharge machining; Inconel-800; surface roughness; energy dispersive x-ray; surface cracks; crater.

INTRODUCTION

Inconel-800 is an iron-nickel-chromium alloy having ample resistance to carburization and oxidation at elevated temperatures as well as moderate strength. It is especially advantageous for high-temperature equipment in the petrochemical industry, heat exchangers, furnace components and electric range heating-element sheathing. The unique properties of the Inconel-800 contain the power to keep high strength and outstanding surface stability. Machining of such material is very difficult using conventional methods of machining because of these characteristics and the machining can be easily done by using different non-conventional machining techniques.

In this frame, electrical discharge machining (EDM) is unitary of non-conventional machining method that can be well used for the machining of complex geometrical form [1]. In spite of the capability to the machine fundamentally any electrically conductive material, the applications of EDM is barred to a few industries,

due to poor productivity and surface quality of machined components. In the past few years, researchers have advanced new modifications to EDM for improving its performance [2, 3]. PMEDM has one of the progressive methods in the flank of the augmentation of the capabilities of EDM. In this process, a fine powder of appropriate material is mixed into the EDM oil so that the spark gap is filled up with additive conductive particles. The electrically conductive additive particles detract the insulating vigor of the dielectric fluid so that the process becomes more static and thus reforming the machining rate and surface finish by Gudur et al. [4]. Before actual experimentation, Pilot experimentation was carried out by using one factor at a time approach for the selection of input process parameters and their levels i.e. current, pulse on-time, pulse off-time. Design of experiments analysis has been carried out by using RSM approach. After that analyzed the results for different composition of powder based dielectric and effect of different composition were studied on the different response parameters considered. The surface integrity of machined surfaces will be analyzed through scanning electron microscope (SEM), and Energy dispersive spectrography (EDS).

Compared the EDM characteristics, i.e. SR and material removal rate obtained by using kerosene dielectric and mixtures of deionized water with abrasive powder and concluded that aluminum as a powder additive improved the surface roughness as compared to other powder additives [5]. Uno et al. [6], added nickel as a powder additive in the EDM oil while performing the experiments on aluminum bronze work specimen and obtained a good surface finish as compared to conventional EDM. Wu et al. [7], mixed aluminum powder in the EDM oil and reported that a more apparent discharge distribution effect which resulted in an SR value of less than 0.2 μm . Tzeng and Chen. [8], conducted experiments on SKD-11 steel with chromium, aluminum, silicon carbide and copper powders and found that aluminum powder provide the best surface finish followed by chromium, whereas copper powder produced the worst surface characteristics. Powder additive properties such as density, thermal conductivity and electrical resistivity impressed the performance. Klocke et al. [9], compared the performance of standard dielectric EDM with aluminum powder-mixed dielectric and found that a larger plasma channel in contrast to the standard dielectric. Zhao et al. [10] performed the experiments on powder-mixed EDM for the response, i.e. machining effectiveness and SR. Reported that powder-mixed EDM clearly improved the responses as compared with conventional EDM. Talla et al. [3], investigated the influence of various powders (aluminum, graphite, silicon) suspended dielectrics and machining parameters on EDM characteristics of Inconel-625. Found that powder properties play a vital role in changing the machining performance and the quality of the machined surface. Among the three powders, silicon powder has a significant effect on surface finish and a least radial overcoat. Kumar [11] and Kumar et al. [12], developed mirror-like surface finish on the surface of AISI-D2 die steel by EDM using carbon nanotubes (CNTs). To analyse the surface characteristics of AISI-D2 die steel, carbon nanotubes are mixed in the EDM oil in defining proportions. Results indicated that the suitable addition of CNTs into EDM oil hikes the machining rate and reduction in SR. Jabbaripour et al. [13] used four levels of current and three levels of on time in their study. The graph is plotted between four points and three points for the output characteristics.

Literature review indicated that a very limited work has been reported on the machining of Inconel-800 with powder particles, i.e. tungsten carbide, cobalt and boron carbide. Also, the effect of tool material, i.e. copper, copper-chromium, and graphite on Inconel-800 material has not been explored. The aim of the present study is to

investigate the effect of tool material along with powder particles mixed in EDM oil on surface characteristics for Inconel-800 material.

EXPERIMENTAL PROCEDURE

Materials

The material used for the experiments was Inconel-800. Samples were rectangular type with dimensions of 150×15×6 mm. The chemical composition of work specimen and tool electrode as shown in Table 1, while mechanical properties of Inconel-800 material as shown in Table 2.

Sanjeev et al. [12], found that copper, copper-chromium has a high melting point and high electrical conductivity. Khazraji et al. [14], reported that graphite is also most widely applied because of its wide industrial applications. Therefore, copper, copper-chromium and graphite were selected as tool electrodes with ϕ 12 mm and 40 mm length. The tool electrodes of copper-chromium, graphite and copper as shown in Figure 1 (a), (b) and (c) while the workpiece specimen after machining is shown in Figure 1 (d).

Table 1. Chemical composition of work specimen and tool electrode material.

| Elements | Work material | | Electrode material | |
|----------|---------------|----------|--------------------|--|
| | Inconel-800 | Copper | Copper- chromium | |
| Ni | Base material | 0.0083 | 0.0104 | |
| Fe | 39.5 | 0.109 | 0.0319 | |
| Cu | < 0.75 | 99.7 | 98.4 | |
| Si | < 1 | < 0.0050 | < 0.0050 | |
| Cr | 20.5 | 0.0061 | 1.36 | |
| Al | – | < 0.0020 | < 0.0020 | |
| S | < 0.015 | < 0.0020 | < 0.0020 | |
| Bi | – | < 0.0050 | < 0.0050 | |
| Sb | – | < 0.0050 | 0.0072 | |
| Zn | – | 0.0148 | < 0.0050 | |
| Pb | – | 0.0206 | 0.0118 | |
| Sn | – | 0.0356 | < 0.0050 | |
| Mn | – | 0.005 | 0.006 | |

Table 2. Mechanical properties of Inconel-800.

| Density | Melting Point | Yield strength | Tensile Strength | Elongation |
|------------------------|---------------|----------------|------------------|------------|
| 7.94 g/cm ³ | 1385 °C | 205- MPa | 520- MPa | 30% |

Process Parameters

There are a large number of input process parameters to be considered within the EDM process for determining the optimal process parameters. Considering the related studies, it was concluded that process parameters such as discharge current, T_{on} , T_{off} , electrodematerial and powder concentration have a clear influence on the EDM performance [13]. Before performing the main EDM tests, pilot experiments have been

done. The pilot experiments were completed with the addition of tungsten carbide, cobalt and boron carbide powder ranging from 1 to 20 g/l into the dielectric fluid to study the effect of SR [15, 16].

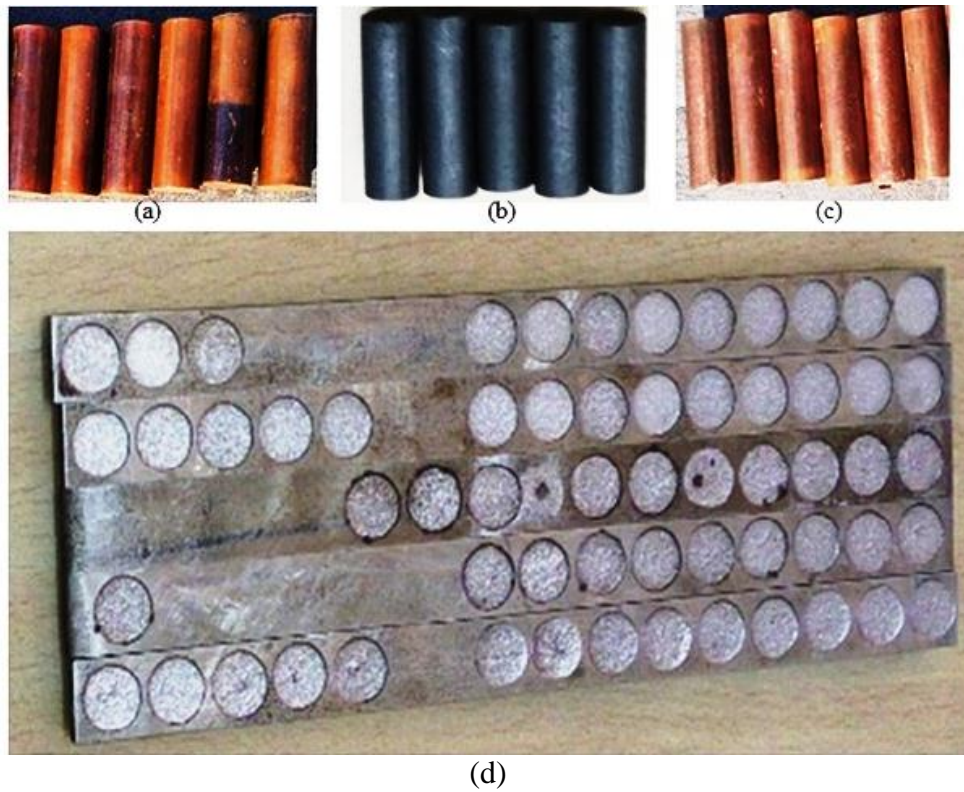


Figure 1. Tool electrodes of (a) copper-chromium, (b) graphite and;(c) copper. (d) Inconel-800 workpiecesafter machining.

It was observed that at 6 g/l tungsten carbide, cobalt and boron carbide powder concentration resulted better in SR. Hence, for main experimentation, the powder concentration is selected at 6 g/l. The range selected for the discharge current, T_{on} and T_{off} is based on pilot experiments and literature. In this study, these three main EDM parameters were selected as input parameters along with tool material (copper, copper-chromium, graphite) and powder particles (tungsten carbide, cobalt and boron carbide). So total five input parameters were selected and the level of each parameter was three. The working range of the input parameters and their level is shown in Table 3.

Table 3. Input parameters and their levels.

| Input factors | Current, I_p (A) | Pulse on-time, T_{on} (μ s) | Pulse off-time, T_{off} (μ s) | Tool material | Powder (g) (Suspended particles) |
|---------------|--------------------|------------------------------------|--------------------------------------|-----------------|----------------------------------|
| Symbol | A | B | C | D | E |
| Level I | 4 | 60 | 30 | Copper | Tungsten-carbide |
| Level II | 8 | 90 | 45 | Copper-chromium | Cobalt |
| Level III | 12 | 120 | 60 | Graphite | Boron-Carbide |

Experimental Setup

A series of experiments were conducted on a die sinking EDM machine (Model OSCARMAX S 645) at the Central Institute of Hand Tools, Jalandhar-Punjab-INDIA. The EDM machine set-up and powder mixing system for EDM is as shown in Figure 2 (a) and (b). The work specimen was firmly clamped in the vice and absorbed in EDM oil. In this experimental study, spark erosion 450EDM oil was used as a dielectric fluid because of its high dielectric strength, high flash point and less surface tension. Forty-six experiments is as shown in Table 4.

The experiments were conducted as per RSM methodology. In each experiment a hole is machined to a depth of 0.5 mm. Before machining, the work specimen and electrodes were cleaned with acetone and bright with emery papers. Positive polarity was used during the experiments as recommended in [2, 21].

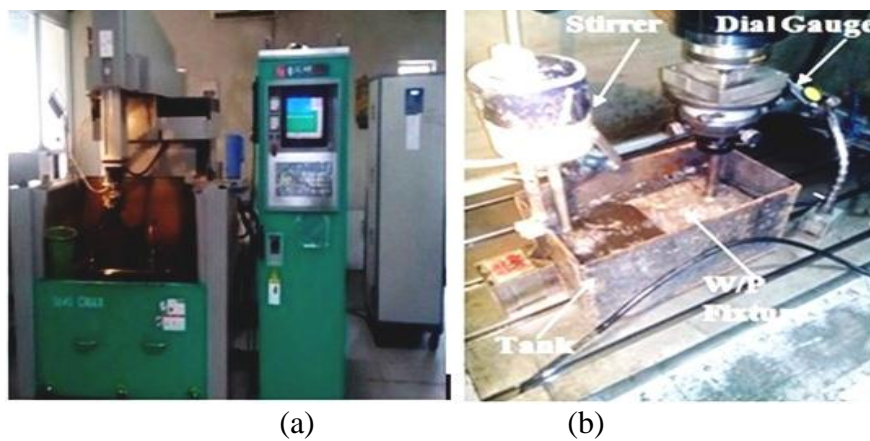


Figure 2. Experimental setup for(a) EDM machining and; (b) Powder mixing system.

Table 4. Design of experiments.

| Run | Current (A) | T_{on} (μ s) | T_{off} (μ s) | Tool Material | Powder |
|-----|-------------|---------------------|----------------------|---------------|--------|
| 1 | 4 | 90 | 60 | Cu-Cr | Co |
| 2 | 8 | 90 | 45 | Cu-Cr | Co |
| 3 | 8 | 90 | 60 | Gr | BC |
| 4 | 8 | 90 | 45 | Cu | WC |
| 5 | 8 | 90 | 30 | Cu-Cr | BC |
| 6 | 8 | 120 | 30 | Cu-Cr | Co |
| 7 | 8 | 90 | 60 | Cu-Cr | BC |
| 8 | 8 | 90 | 60 | Cu | Co |
| 9 | 4 | 90 | 45 | Cu | Co |
| 10 | 8 | 90 | 45 | Cu-Cr | Co |
| 11 | 8 | 90 | 45 | Cu-Cr | Co |
| 12 | 8 | 90 | 45 | Gr | WC |
| 13 | 8 | 90 | 30 | Gr | Co |
| 14 | 12 | 90 | 30 | Cu-Cr | Co |
| 15 | 8 | 90 | 30 | Cu | Co |
| 16 | 12 | 90 | 45 | Cu-Cr | BC |

| | | | | | |
|----|----|-----|----|-------|----|
| 17 | 12 | 90 | 60 | Cu-Cr | Co |
| 18 | 8 | 120 | 45 | Cu-Cr | WC |
| 19 | 4 | 90 | 45 | Gr | Co |
| 20 | 12 | 90 | 45 | Gr | Co |
| 21 | 8 | 120 | 60 | Cu-Cr | Co |
| 22 | 4 | 90 | 45 | Cu-Cr | BC |
| 23 | 8 | 90 | 45 | Gr | BC |
| 24 | 8 | 120 | 45 | Cu | Co |
| 25 | 12 | 60 | 45 | Cu-Cr | Co |
| 26 | 8 | 90 | 45 | Cu-Cr | Co |
| 27 | 8 | 90 | 60 | Cu-Cr | WC |
| 28 | 4 | 90 | 30 | Cu-Cr | Co |
| 29 | 12 | 90 | 45 | Cu | Co |
| 30 | 4 | 120 | 45 | Cu-Cr | Co |
| 31 | 8 | 120 | 60 | Cu-Cr | Co |
| 32 | 12 | 90 | 45 | Cu-Cr | WC |
| 33 | 8 | 90 | 45 | Cu | BC |
| 34 | 8 | 90 | 45 | Cu-Cr | Co |
| 35 | 8 | 60 | 45 | Cu-Cr | WC |
| 36 | 12 | 120 | 45 | Cu-Cr | Co |
| 37 | 8 | 120 | 45 | Gr | Co |
| 38 | 8 | 120 | 45 | Cu-Cr | BC |
| 39 | 8 | 90 | 45 | Cu-Cr | Co |
| 40 | 8 | 90 | 30 | Cu-Cr | WC |
| 41 | 8 | 60 | 60 | Cu-Cr | Co |
| 42 | 4 | 60 | 45 | Cu-Cr | Co |
| 43 | 8 | 60 | 45 | Cu-Cr | BC |
| 44 | 8 | 60 | 45 | Gr | Co |
| 45 | 8 | 60 | 45 | Cu | Co |
| 46 | 4 | 90 | 45 | Cu-Cr | WC |

RESULTS AND DISCUSSION

Determination of Main Effects on Surface Roughness

Table 5 shows the result of the experiments to be conducted as per the RSM methodology. Equation (3) and (4) shows the connection between machining parameters and response in coded as well as in actual form respectively. According to analysis of variance (ANOVA) as shown in Table 6 (before elimination) factors A, C, D, E and two interactions factor AC and CE, i.e. discharge current, T_{off} , tool material, powder particles and interaction ($I_p \times T_{off}$, $T_{off} \times$ powder particles) are significant for surface roughness. The p value for lack of fit is 0.2909 indicating that this model sufficiently fits the data.

The “Pred R-Squared” of 0.93 is in proper contract with the “Adj R-Squared” of 0.96. “AdeqPrecision” measures the signal to noise ratio. To fit the quadratic model for SR suitable, non vital terms was removed by backward elimination. The backward elimination procedure is applied to get rid of the non-vital terms so that the quadratic model to be fit. Reduced model for SR is as shown in Table 7. After backward

elimination, the results indicate that the model is validated having R-Squared and Adjusted R-Squared as 97 % and 96 %, respectively.

From the main effect plots based on Figure 3 (a), it has been found that whenever current was increased from 4 to 12 A, the SR hikes significantly. The increment of SR was approximately from 4.23 to 12.57 μm. When T_{off} reduced from 60 to 30 μs, it showed the most significant effect on SR i.e., from 7.10 to 9.23 μm as shown in Figure 3 (c). The same trend was observed by [22,23]. As for pulse on-time, a slight increment of surface roughness occurred when pulse on-time was hiked from 60 to 120 μs with 9.19 to 10.19 μm as shown in Figure 3 (b).

Table 5. Surface roughness of samples after experimentation.

| | | | | | | | | | | |
|------------|------|-------|-------|-------|-------|-------|-------|-------|-------|-------|
| Run no. | 1 | 2 | 3 | 4 | 5 | 6 | 7 | 8 | 9 | 10 |
| R-1 | 3.50 | 9.92 | 6.45 | 8.89 | 9.16 | 9.16 | 5.90 | 6.88 | 3.01 | 8.72 |
| R-2 | 4.59 | 9.92 | 6.48 | 7.89 | 11.21 | 9.45 | 6.11 | 6.78 | 3.91 | 8.72 |
| R-3 | 3.51 | 7.17 | 5.08 | 7.29 | 9.36 | 9.67 | 5.11 | 6.14 | 4.78 | 8.94 |
| Mean Value | 3.87 | 9.00 | 6.00 | 8.02 | 9.91 | 9.43 | 5.71 | 6.60 | 3.90 | 8.79 |
| Run no. | 11 | 12 | 13 | 14 | 15 | 16 | 17 | 18 | 19 | 20 |
| R-1 | 8.70 | 10.33 | 10.68 | 13.71 | 6.71 | 10.39 | 9.48 | 11.66 | 4.15 | 13.42 |
| R-2 | 8.76 | 10.38 | 10.70 | 13.70 | 7.10 | 10.19 | 9.48 | 10.56 | 3.10 | 13.60 |
| R-3 | 9.21 | 11.51 | 11.59 | 13.26 | 7.20 | 9.22 | 8.05 | 10.57 | 3.28 | 13.63 |
| Mean Value | 8.89 | 10.74 | 10.99 | 13.56 | 7.00 | 9.93 | 9.00 | 10.91 | 3.51 | 13.55 |
| Run no. | 21 | 22 | 23 | 24 | 25 | 26 | 27 | 28 | 29 | 30 |
| R-1 | 9.16 | 3.54 | 7.89 | 9.07 | 12.06 | 10.32 | 8.71 | 3.25 | 10.52 | 4.33 |
| R-2 | 9.10 | 3.70 | 7.88 | 8.42 | 13.50 | 10.32 | 8.84 | 3.07 | 9.70 | 4.56 |
| R-3 | 8.15 | 3.71 | 7.89 | 8.63 | 13.66 | 9.34 | 8.87 | 2.68 | 10.80 | 4.57 |
| Mean Value | 8.80 | 3.65 | 7.89 | 8.71 | 13.07 | 9.99 | 8.81 | 3.00 | 10.34 | 4.49 |
| Run no. | 31 | 32 | 33 | 34 | 35 | 36 | 37 | 38 | 39 | 40 |
| R-1 | 8.99 | 14.05 | 8.19 | 10.09 | 10.40 | 15.03 | 10.71 | 10.56 | 8.71 | 8.38 |
| R-2 | 8.61 | 13.98 | 8.01 | 9.31 | 10.03 | 14.09 | 10.03 | 9.35 | 9.46 | 8.28 |
| R-3 | 9.65 | 14.99 | 8.51 | 9.38 | 10.04 | 14.10 | 9.03 | 9.60 | 8.81 | 7.23 |
| Mean Value | 9.08 | 14.34 | 8.23 | 9.59 | 10.16 | 14.41 | 9.92 | 9.84 | 8.99 | 7.96 |
| Run no. | 41 | 42 | 43 | 44 | 45 | 46 | | | | |
| R-1 | 5.90 | 4.05 | 8.57 | 10.64 | 7.97 | 5.88 | | | | |
| R-2 | 6.01 | 3.80 | 7.49 | 9.60 | 7.09 | 5.01 | | | | |
| R-3 | 6.10 | 4.44 | 7.69 | 9.09 | 7.35 | 4.03 | | | | |
| Mean Value | 6.00 | 4.09 | 7.92 | 9.78 | 7.47 | 4.97 | | | | |

$$Ra = +9.18 + 4.17 \times A + 0.50 \times B - 1.06 \times C + 0.76 \times D - 0.80 \times A^2 + 0.49 \times B^2 - 1.04 \times C^2 - 0.55 \times D^2 - 1.36 \times A \times E + 0.90 \times B \times C - 1.15 \times C \times D - 1.26 \times C \times E - 0.77 \times D \times E \quad (3)$$

$$Ra = -5.69 + 2.86 \times \text{current} - 0.17 \times T_{on} + 0.34 \times T_{off} + 2.39 \times \text{tool} + 4.52 \times \text{powder} - 0.50 \times \text{current}^2 + 5.44 \times 10^{-4} \times T_{on}^2 - 4.61 \times 10^{-3} \times T_{off}^2 - 0.55 \times \text{tool}^2 - 0.022 \times \text{current} \times T_{off} \quad (4)$$

$$+0.22 \times \text{current} \times \text{tool} - 0.19 \times \text{current} \times \text{powder} + 1.99 \times 10^{-3} \times T_{\text{on}} \times T_{\text{off}} - 0.77 \times T_{\text{off}} \times \text{tool} - 0.08 \times T_{\text{off}} \times \text{powder} - 0.76 \times T_{\text{off}} \times \text{tool} - 0.08 \times T_{\text{off}} \times \text{powder} - 0.76 \times \text{tool} \times \text{powder}$$

Table 6. Analysis of variance for surface roughness (before elimination).

| Source | Sum of Squares | DF | Mean Square | F-Value | Prob > F | |
|---------------------|----------------|----|----------------------|---------|----------|-----------------|
| Model | 370.04 | 20 | 18.5 | 65.45 | < 0.0001 | significant |
| A | 278.13 | 1 | 278.13 | 983.9 | < 0.0001 | |
| B | 3.59 | 1 | 3.59 | 12.72 | 0.0015 | |
| C | 16.28 | 1 | 16.28 | 57.59 | < 0.0001 | |
| D | 9.14 | 1 | 9.14 | 32.34 | < 0.0001 | |
| E | 10.31 | 1 | 10.31 | 36.47 | < 0.0001 | |
| A2 | 5.75 | 1 | 5.75 | 20.36 | 0.0001 | |
| B2 | 1.97 | 1 | 1.97 | 6.97 | 0.0141 | |
| C2 | 9.4 | 1 | 9.4 | 33.28 | < 0.0001 | |
| D2 | 2.78 | 1 | 2.78 | 9.84 | 0.0043 | |
| E2 | 0.01 | 1 | 0.01 | 0.04 | 0.834 | |
| AB | 0.22 | 1 | 0.22 | 0.78 | 0.3851 | |
| AC | 7.35 | 1 | 7.35 | 26.01 | < 0.0001 | |
| AD | 3.24 | 1 | 3.24 | 11.48 | 0.0023 | |
| AE | 2.38 | 1 | 2.38 | 8.42 | 0.0076 | |
| BC | 2.78 | 1 | 2.78 | 9.85 | 0.0043 | |
| BD | 0.29 | 1 | 0.29 | 1.05 | 0.3143 | |
| BE | 0.33 | 1 | 0.33 | 1.19 | 0.2857 | |
| CD | 5.25 | 1 | 5.25 | 18.59 | 0.0002 | |
| CE | 6.36 | 1 | 6.36 | 22.5 | < 0.0001 | |
| DE | 2.34 | 1 | 2.34 | 8.3 | 0.008 | |
| Residual | 7.06 | 25 | 0.28 | | | |
| Lack of Fit | 5.9 | 19 | 0.31 | 1.6 | 0.2909 | Not significant |
| Pure Error | 1.16 | 6 | 0.1938806 | | | |
| Cor Total | 377.11 | 45 | | | | |
| R ² | 0.98 | | Pred. R ² | 0.93 | | |
| Adj. R ² | 0.96 | | Adeq. Precision | 31.21 | | |

Table 7. Analysis of variance for surface roughness (after elimination).

| Source | Sum of Squares | DF | Mean Square | F-Value | Prob > F | |
|--------|----------------|----|-------------|---------|----------|-------------|
| Model | 369.17 | 16 | 23.07 | 84.32 | < 0.0001 | significant |
| A | 278.13 | 1 | 278.13 | 1016.47 | < 0.0001 | |
| B | 3.61 | 1 | 3.61 | 13.21 | 0.0011 | |
| C | 16.26 | 1 | 16.26 | 59.45 | < 0.0001 | |
| D | 9.14 | 1 | 9.14 | 33.41 | < 0.0001 | |
| E | 10.31 | 1 | 10.31 | 37.68 | < 0.0001 | |
| A2 | 6.06 | 1 | 6.06 | 22.16 | < 0.0001 | |
| B2 | 2.2 | 1 | 2.2 | 8.06 | 0.0082 | |
| C2 | 9.91 | 1 | 9.91 | 36.22 | < 0.0001 | |

| | | | | | | |
|---------------------|--------|----|----------------------|-------|----------|-----------------|
| D2 | 2.89 | 1 | 2.89 | 10.59 | 0.0029 | |
| AC | 7.35 | 1 | 7.35 | 26.87 | < 0.0001 | |
| AD | 3.24 | 1 | 3.24 | 11.86 | 0.0018 | |
| AE | 2.38 | 1 | 2.38 | 8.7 | 0.0062 | |
| BC | 2.78 | 1 | 2.78 | 10.16 | 0.0034 | |
| CD | 5.25 | 1 | 5.25 | 19.2 | 0.0001 | |
| CE | 6.36 | 1 | 6.36 | 23.24 | < 0.0001 | |
| DE | 2.34 | 1 | 2.34 | 8.57 | 0.0066 | |
| Residual | 7.93 | 29 | 0.27 | | | |
| Lack of Fit | 6.77 | 23 | 0.29 | 1.51 | 0.3166 | Not significant |
| Pure Error | 1.16 | 6 | 0.19 | | | |
| Cor Total | 377.11 | 45 | | | | |
| R ² | 0.97 | | Pred. R ² | 0.94 | | |
| Adj. R ² | 0.96 | | Adeq. Precision | 35.35 | | |

From Figure 3 (d), it is clear that among the three tool electrode material, copper has significantly effected on SR, while among the three powder particles, boron carbide has a significant effect on the SR as illustrated in Figure 3 (e). With the use of tungsten carbide as a powder particle, surface roughness was 9.98 μm , while with boron carbide surface roughness was 8.37 μm . With the increase of current, longer the spark is sustained and more material is removed from the work specimen. Therefore craters formed on the surface will be deeper, resulting an increase in SR. In order to obtain better SR during PMEDM of Inconel-800, the optimum parameter combination obtained is current at 4 A, $T_{\text{on}} = 90 \mu\text{s}$, $T_{\text{off}} = 60 \mu\text{s}$, copper as a tool electrode material and boron carbide as a suspended powder.

Figure 3 (f) shows the perturbation plot to compare the effect of all the facts at a specific point in the design area. Basically, it provides silhouette views of the response surface. Factor A, C, D and E show the slope means the response is sensitive to that factor. In addition to this normal plot of residuals and residual versus predicted plots have also been drawn. The data are normally distributed as shown in Figure 4 (a). It has also been observed from Figure 4 (b) that all the experimental results are nearly very close to expected values.

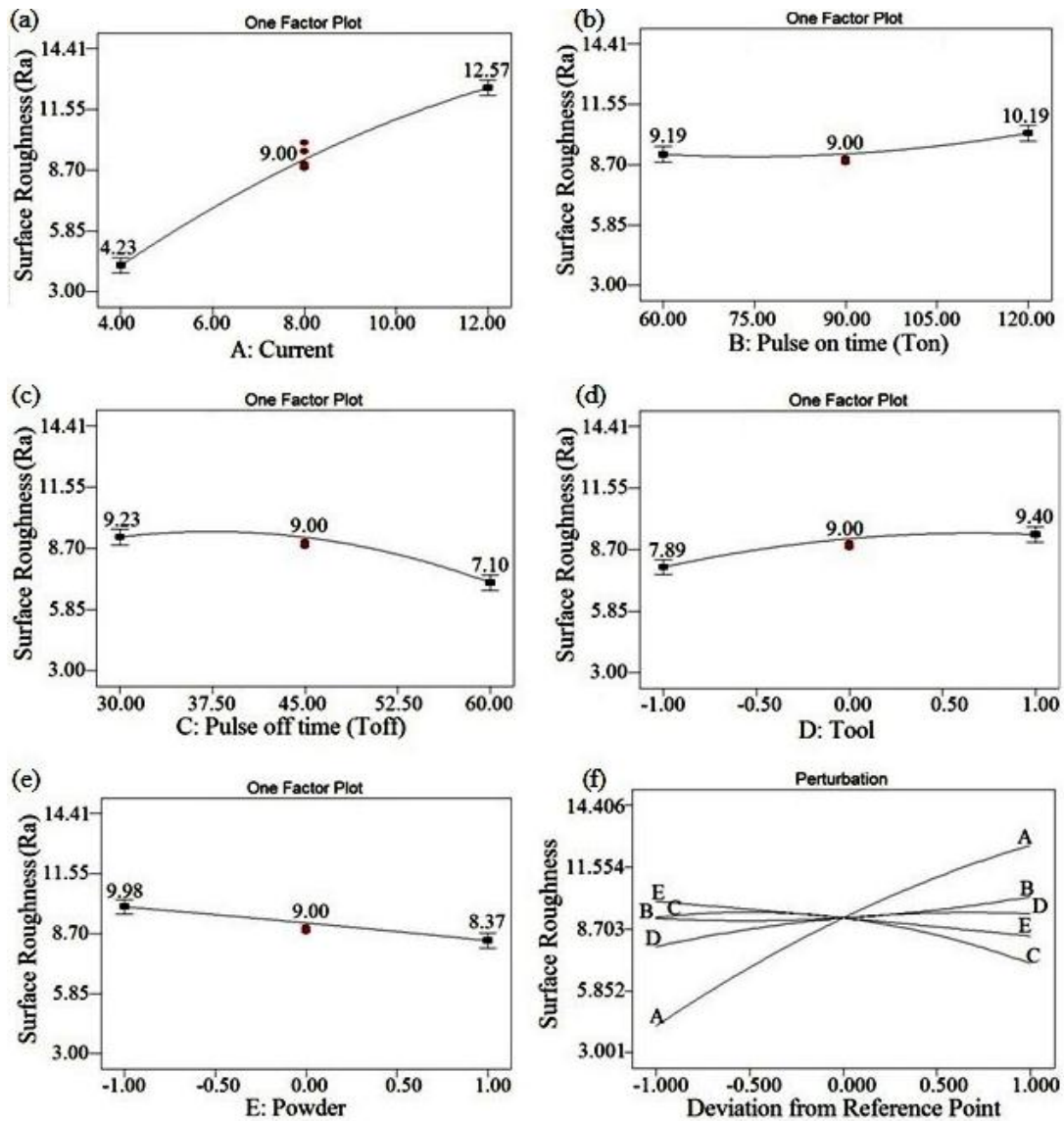


Figure 3. One factor plots for surface roughness.

Determination of Interaction Effects on Surface Roughness

Based on Table 5, there are two interactions have been involved ($I_p \times T_{off}$, $T_{off} \times$ powder particles) as shown in Figure 4 (c) and (d). The “Prob>F” value of both interactions, i.e. $I_p \times T_{off}$ and $T_{off} \times$ powder particles are <0.0001 . It is clear from the Figure 4 (c) that when current increased from 4 to 12 A and T_{off} vary from 30 to 60 μ s then SR hiked from 2.88 to 11.17 μ m.

When current increased from 4 to 12 A along with boron carbide as a powder additive surface roughness vary from 4.15 to 8.40 μ m, while along with tungsten carbide as a powder additive; it is changed from 4.15 to 11.61 μ m as shown in Figure 4 (d). The SR increased when peak current increased along with pulse on-time due to the longer time for machining the work specimen.

The interaction graph between current and powder particles are as shown in Figure 4 (e). It is clear from the Figure 4 that with the same value of current, powder

particles has more effect on SR. The same effect is observed for the contour plot of current and powder as shown in Figure 4 (f).

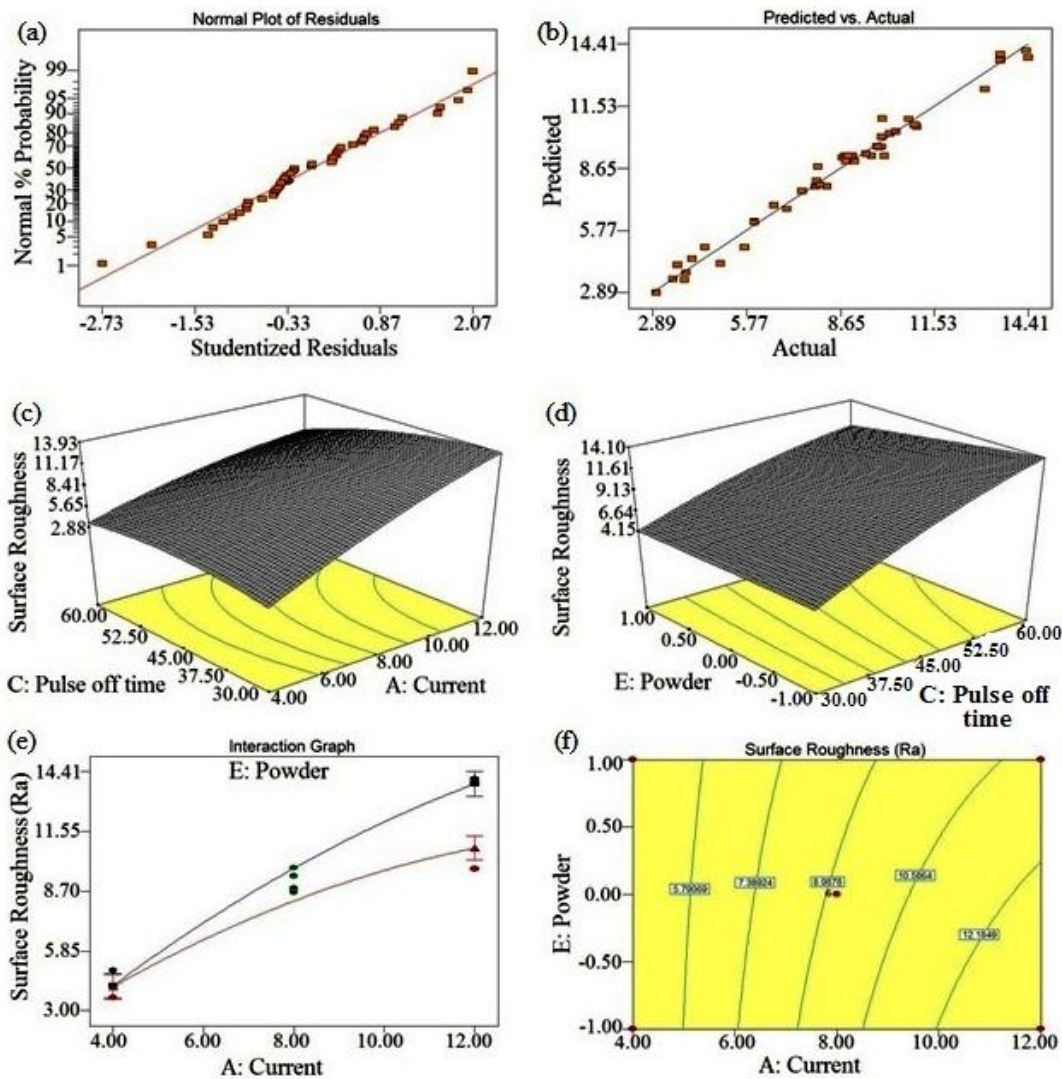


Figure 4. Response surface plots: (a) normal probability residual plot; (b) predicted v/s actual plot; (c), (d), 3D surface plot for SR; (e) interaction plot for SR and (f) contour plot for SR.

Microstructure Analysis

After PMEDM operations, surfaces of Inconel-800 has major microstructural changes after PMEDM. The characteristics of machined surface are represented by the formation of surface cracks, metallurgical changes on the machined surface. Current, T_{on} , electrode polarity, electrode, workpiece material and powder mixed dielectric medium are the main factors which are accountable for affecting the surface quality of the machined specimen during the machining with EDM [1],[24]. For the intent of scrutiny, three trials for current setting, namely (i) 4A, (ii) 8A and (iii) 12A along with three different tool materials and three powder particles, were analyzed in detail.

SEM micrograph of Inconel-800 machined with 8A current, $90\mu s$ T_{on} , $60\mu s$ T_{off} , graphite as a tool material and boron carbide as a powder additive in the EDM oil as

illustrated in Figure 5(a), (d) and (g) along with the magnification of 500 \times , 2000 \times and 5000 \times respectively. The Figure 5 (a) shows the formation of debris, crater and fragments, but with higher magnification, subsurface cracks with debris and deep cracks can be noticed on the surface as illustrated in Figure 5 (d) and (g). Figure 5 (b, e and h) shows the micrographs with the machining condition at 12A current, 60 μ s T_{on} , 45 μ s T_{off} , graphite as a tool material and cobalt as a powder additive in the dielectric fluid. Micro cracks along with debris and crater are shown in Figure 5 (b). With the critical examination of highly magnified images, surface cracks and deep cracks were noticed on the surface as shown in Figure 5 (e) and (h). Figure 5 (c), (f) and (i) shows the micrographs with the machining condition at 4 A current, 90 μ s T_{on} , 45 μ s T_{off} , copper-chromium as a tool material and tungsten carbide as a powder additive in the dielectric fluid. Micro-cracks, material pull out and debris were noticed on the surface as shown in Figure 5 (c) but with higher magnification surface and deep cracks can be noticed on the surface as shown in Figure 5 (f) and (i). The micro graphs presented in these figures exposed that surface maybe caused by an unequal fusing structure, micro cracks, pock marks, craters, globules of debris, sub surface cracks and fragments. It was noticed from Figure 5 (a), (b), (d), (e), (g) and (h) that PMEDM surface produces large uneven topography and defects included debris, fragments, deep craters, pockmarks, surface cracks, sub-surface crack and micro-cracks when compared with Figure 5 (c), (f) and (i).

The peak current is the most vital parameter that is responsible for deterioration of the surface texture. This is due to the reason that with the hike of current high discharge energy is transferred to the machining area, so that melting and evaporation take place, resulting in the formation of a small crater [15]. Also, deep craters were formed by the successive electrical discharge and vaporized the work specimen [25]. The results of this study agree with [24].

EDX Analysis

With the continuous flow of dielectric fluid, the metal particles coming from electrode to workpiece are flushed out. Some material particles are left on the machined specimen surface because of the particles that cannot be transported completely of the discharge gap. The output of EDX analysis is a plot of how frequently an X-ray is received in each energy level [26]. EDX results show the improved quality and quantity values of elemental composition of the Inconel-800 work piece. Figure 6 (a) and (b) compares the EDX pattern of before and after machining samples, in order to investigate the chemical composition.

Before PMEDM machining, the weight percentage of elements are C= 12.33, O= 2.1, Cr= 17.16, Fe= 41.48 and Ni= 26.93 as shown in Figure 6 (a). With PMEDM at different machining conditions, weight, the percentage of element changes to C= 12.33 to 19.12, O= 2.1 to 3.93, Cr= 17.16 to 16.64, Fe= 41.48 to 37.95 and Ni= 26.93 to 22.36 as illustrated in Figure 6(b). The hike in the percentage of oxygen in Inconel-800 probably was due to oxidation as a result of high temperature involved in the process. Also, when graphite as a tool electrode along with boron carbide powder (concentration) is added into the EDM oil, there was an increase in the carbon content and during the machining process this carbon dissolves in the EDM oil and on the metal surface.

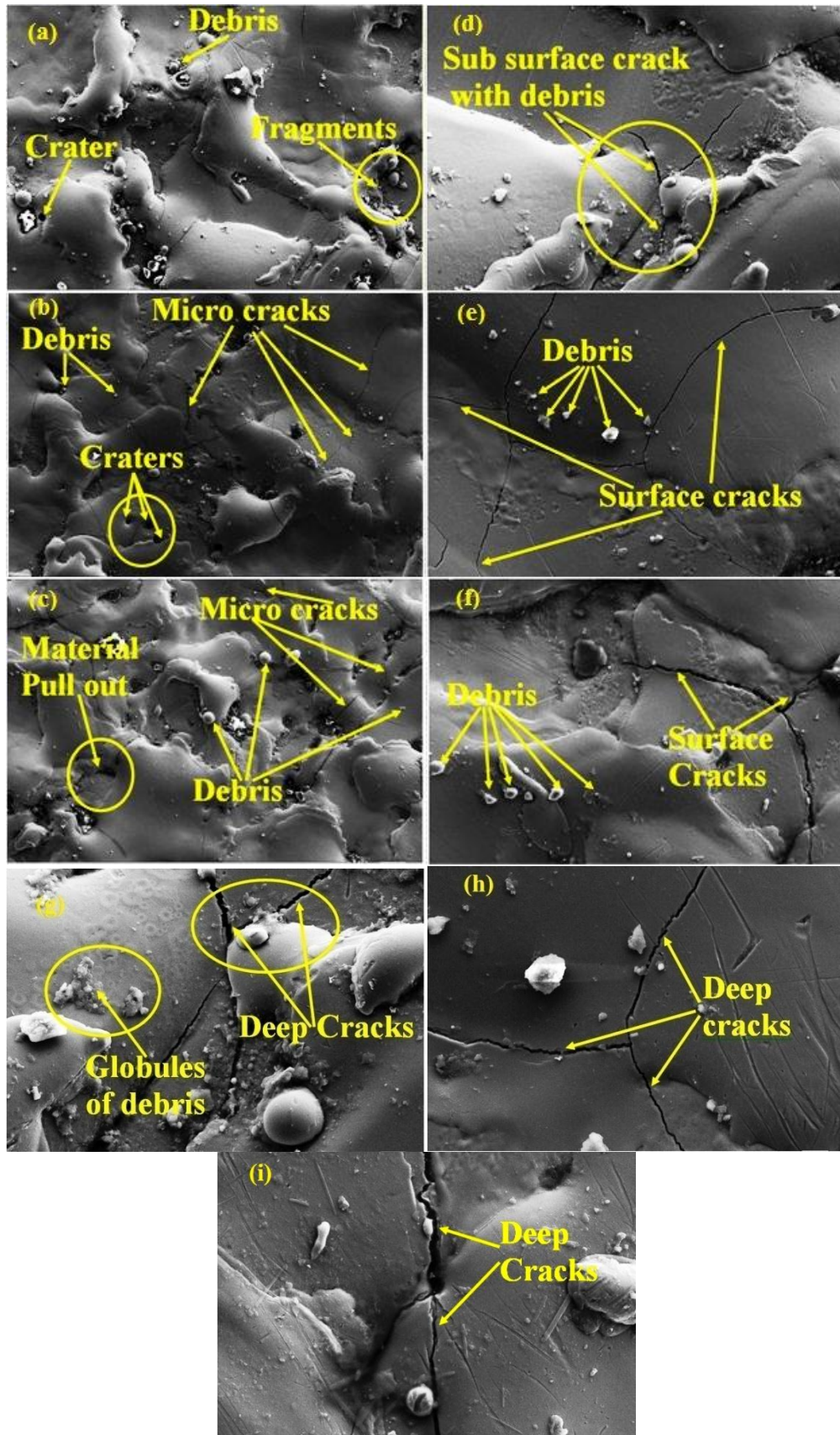
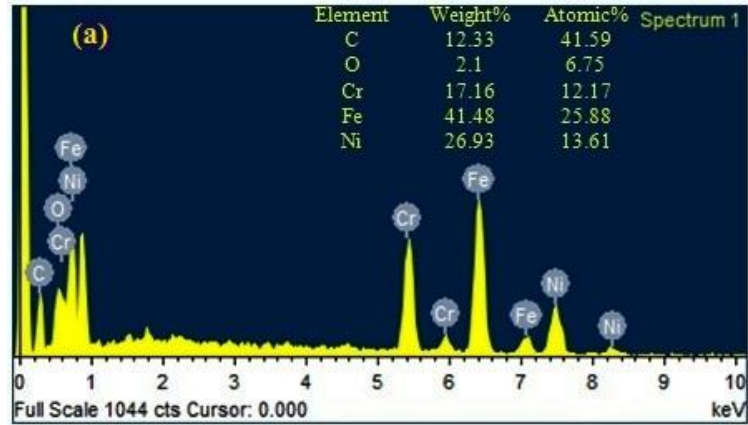
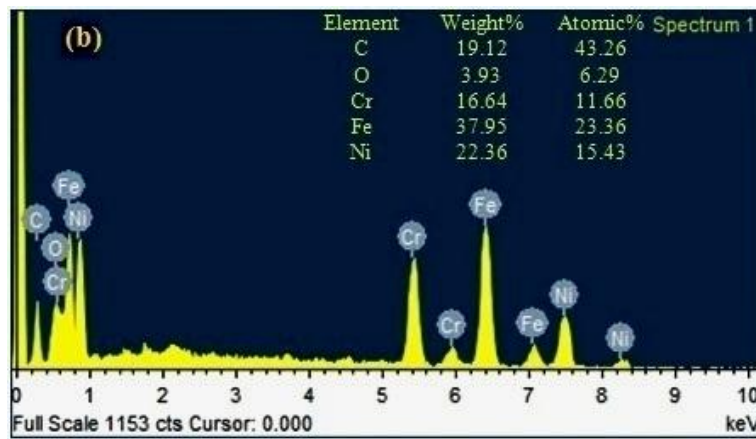


Figure 5. SEM micrographs of samples from run no. (a),(d) 3, (b),(e) 44, (c),(f) 46, (g) 3, (h) 44 and; (i) 46.



(a) before machining.



(b) after machining

Figure 6. EDX analysis of Inconel-800.

CONFIRMATION EXPERIMENT

Three confirmation experiment has been performed for surface roughness. For the confirmation test, values of selected process variables lie in the ranges for which the formula was derived [16]. The data for the confirmation run and predicted designed for SR is shown in Table 8 and found that the calculated error is small. The error between experimental and expected values for SR is lying within -8.55% to 5.1%, respectively. Obviously, this confirms the superior reproducibility of the experimental outcomes.

Table 8. Conformation test.

| Sample | Machining Conditions | | | | | Surface Roughness (μm) | | |
|--------|----------------------|---------------------------------------|--|------------------|-----------|-------------------------------------|-------------|-----------|
| | Current (A) | T _{on} , B (μs) | T _{off} , C (μs) | Tool material, D | Powder, E | Exp. value | Pred. value | Error (%) |
| 1 | 4 | 60 | 45 | Cu-Cr | Co | 4.09 | 4.44 | -8.55 |
| 2 | 8 | 90 | 45 | Cu | BC | 8.23 | 7.81 | 5.1 |
| 3 | 12 | 90 | 45 | Cu-Cr | WC | 14.34 | 14.1 | 1.67 |

CONCLUSION

The quadratic model for SR has been developed to correlate the machining process variables: current, T_{on} , T_{off} , tool electrode and powder particles, in the PMEDM process of Inconel-800. To perform experimental work, a Box-Behnken method of RSM has been applied. Based on experimental study, results indicated that SR obtained was ranged from 4.23 μm to 12.57 μm . The SR was most significantly affected by current, T_{off} , tool material and powder particles. The minimum SR was obtained, when the parameters are set as $I_p = 4$ amp, $T_{on} = 60$ μs , $T_{off} = 60$ μs , tool material as a copper and boron-carbide as a powder particles. Surface roughness improves when T_{off} , copper as a tool electrode and boron carbide is used as a powder particle while SR increased with the increase of current. T_{on} has little bit effect on SR. The co-efficient of regression R^2 , adj. R^2 and predicted R^2 obtained for the developed surface roughness is 0.98, 0.96 and 0.93. "Pred R^2 " of 0.93 is in an acceptable contract with the "Adj R^2 " of 0.96. The confirmation test showed that the error between the expected and experimental value of SR is -8.55% to 5.1%, respectively. This confirms validation of results for predicted values and experimental values. It was noticed from the SEM micrographs of machined surfaces that peak current affects the surface structure of machined samples resulting in formation of micro cracks, craters, pockmarks and debris. At lower current and higher T_{off} better surface characteristics may be obtained.

ACKNOWLEDGEMENT

The authors would like to be obliged to Assistant Director, Central Institute of Hand Tools, Jalandhar, Punjab, India, for providing the EDM set-up.

REFERENCES

- [1] Kumar A, Maheshwari S, Sharma C, Beri N. Research Developments in Additives Mixed Electrical Discharge Machining (AEDM): A State of Art Review. *Materials and Manufacturing Process*. 2010; 25: 1166–1180.
- [2] Talla G, Gangopadhyay S, Biswas CK. State of the art in powder-mixed electric discharge machining: A review. *Journal of Engineering Manufacture*. 2016; 1-16.
- [3] Talla G, Gangopadhyay S, Biswas CK. Effect of Powder-Suspended Dielectric on the EDM Characteristics of Inconel 625. *Journal of Materials Engineering and Performance*. 2016; 25: 707-717.
- [4] Gudur S, Potdar VV, Gudur S. A Review on Effect of Aluminum & Silicon Powder Mixed EDM on Response Variables of Various Materials. *International Journal of Innovative Research in Science, Engineering and Technology*. 2014; 12: 17937- 17945.
- [5] Kozak J, Rozenek M, Dabrowski L. Study of electrical discharge machining using powder-suspended working media. *Journal of Engineering Manufacture*. 2003; 217: 1597-1602.
- [6] Uno Y, Okada A, Cetin S. Surface modification of EDMed surface with powder mixed fluid. *Proceedings of the 2nd Int. Conf. on Design and Production of Dies and Molds*. 2001;
- [7] Wu KL, Yan BH, Huang FY, Chen SC. Improvement of surface finish on SKD steel using electro-discharge machining with aluminum and surfactant added

- dielectric. *International Journal of Machine Tools & Manufacture*. 2005; 45: 1195-1201.
- [8] Tzeng Y, Chen F. Investigation into some surface characteristics of electrical discharge machined SKD-11 using powder-suspension dielectric oil. *International Journal of Materials Processing Technology*. 2005; 170: 385-391.
- [9] Klocke F, Lung D, Antonoglou G, Thomaidis D. The effects of powder suspended dielectrics on the thermal influenced zone by electro discharge machining with small discharge energies. *International Journal of Materials Processing Technology*. 2004; 149: 191-197.
- [10] Zhao WS, Meng QG, Wang ZL. The application of research on powder mixed EDM in rough machining. *Journal of Materials Processing Technology*. 2002; 129: 30-33.
- [11] Kumar H. Development of mirror like surface characteristics using nano powder mixed electric discharge machining (NPMEDM). *The International Journal of Advanced Manufacturing Technology*. 2015; 76: 105-113.
- [12] Kumar S, Singh R, Batish A, Singh TP. Study the Surface Characteristics of Cryogenically Treated Tool-Electrodes in Powder Mixed Electric Discharge Machining Process. *Material Science Forum*. 2015; 808: 19-33.
- [13] Jabbaripour B, Sadeghi MH, FaridvandSh, Shabgard MR. Investigating the Effects of EdM Parameters on Surface Integrity, MRR and TWR in Machining of Ti-6Al-4V. *Mach Sci Technol An Int.J.* 2012; 16: 419-444.
- [14] Khazraji A, Amin SA, Ali SM. The effect of SiC powder mixing electrical discharge machining on white layer thickness, heat flux and fatigue life of AISI D2 die steel. *Engineering Science Technology, An International Journal*. 2016; 19: 1400-1415.
- [15] Kolli M, Kumar A. Effect of dielectric fluid with surfactant and graphite powder on Electrical Discharge Machining of titanium alloy using Taguchi method. *Engineering Science Technology, An International Journal*. 2015; 18: 524-535.
- [16] Kansal HK, Singh S, Kumar P. Parametric optimization of powder mixed electrical discharge machining by response surface methodology. *Journal of Material Process Technology*. 2005; 169: 427-436.
- [17] Vikram S, Pradhan SK. Optimization of EDM process parameters: a review. *International Journal of Emerged Technology and Advanced Engineering*. 2014; 4: 345-355.
- [18] Mittal S, Kumar V, Kumar H. Multi-response optimization of process parameters involved in micro-finishing of Al/SiC MMCs by abrasive flow machining process. *Journal of Materials Design and Application*. 2016; 1-14.
- [19] Kung KY, Horng JT, Chiang KT. Material removal rate and electrode wear ratio study on the powder mixed electrical discharge machining of cobalt-bonded tungsten carbide. *The International Journal of Advanced Manufacturing Technology*. 2009; 40: 95-104.
- [20] Muthukumar V, Rajesh N, Venkatasamy R, Sureshbabu A, Senthilkumar N. Mathematical Modeling for Radial Overcut on Electrical Discharge Machining of Incoloy 800 by Response Surface Methodology. *Procedia Materials Science*. 2014; 6: 1674 - 1682.
- [21] Singla YK, Chhibber R, Bansal H, Kalra A. Wear Behaviour of Aluminum Alloy 6061-Based Composite Reinforced With SiC, Al₂O₃, and Red Mud: A Comparative Study.

- [22] Biing HY, Hsien TC, Fuang HY, Long LC. Examination of wire electric discharge machining of Al₂O₃p/6061Al composites. *International Journal of Machine Tools and Manufacturing*. 2005; 45: 251–259.
- [23] Kumar A, Kumar V. Kumar J. Multi-response optimization of process parameters based on response surface methodology for pure titanium using WEDM process. *International Journal of Advanced Manufacturing Technology*. 2013; DOI 10.1007/s00170-013-4861-9.
- [24] Hascalik A, Caydas U. Electric discharge machining of titanium alloy. *Applied Surface Science*. 2007; 253: 9007-9016.
- [25] Lin YC, Tsao CC, Hsu CY, Hung SK, Wen DC. Evaluation of the characteristics of the micro electrical discharge machining process using response surface methodology based on the central composite design. *International Journal of Advanced Manufacturing Technology*. 2012; 62: 1013–1023.
- [26] Patil GN, Brahmankar PK. Some studies into wire electro-discharge machining of alumina particulate-reinforced aluminum matrix composites. *International Journal of Advavced Manufacturing Technology*. 2010; 48: 537–555.